

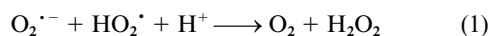
Synthesis, crystal structure and superoxide dismutase activity of a five-co-ordinated manganese(II) complex

Dao Feng Xiang, Chun Ying Duan, Xiang Shi Tan, Qin Wei Hang and Wen Xia Tang *

Coordination Chemistry State Key Laboratory, Coordination Chemistry Institute,
Nanjing University, Nanjing 210093, P.R. China

A five-co-ordinate manganese(II) complex $[\text{Mn}(\text{ntb})(\text{Hsal})][\text{ClO}_4]$, where ntb is tris(benzimidazol-2-ylmethyl)amine and Hsal^- is the anion of salicylic acid (H_2sal), has been prepared and characterized by X-ray crystallography. The manganese adopts a distorted trigonal-bipyramidal co-ordination geometry with a N_4O ligand donor set and bears structural similarities to the active site of manganese superoxide dismutase. The electrochemical properties of the complex were studied in MeCN by cyclic voltammetry. The complex can catalyse the dismutation of superoxide ($\text{O}_2^{\cdot -}$) effectively in the riboflavin–methionine–nitro blue tetrazolium assay.

The superoxide radical anion, a product of cellular respiration, activated polymorphonuclear leukocytes and endothelial cells, has been demonstrated to be a mediator of ischemia, reperfusion injury, inflammatory and vascular diseases.¹ The main lines of defence in mammalian organisms for controlling extra- and intra-cellular superoxide radical anions are the Cu/Zn-, Mn- and Fe-containing superoxide dismutase enzymes.² Superoxide dismutase (SOD) catalyses the dismutation of superoxide radical anions to the non-radical products oxygen and hydrogen peroxide³ [equation (1)] and protects living cells against the



toxicity of hyperoxia. The application of superoxide dismutase as a pharmaceutical has attracted considerable attention.^{4–6} However, SODs have molecular weights too high to cross cell membranes⁷ and can only provide extracellular protection.⁸ In order to circumvent this difficulty, a stable non-toxic, low-molecular-weight metal complex that catalyses the dismutation of superoxide anion might be a suitable alternative to superoxide dismutase in clinical applications^{9–11} with the desirable qualities of low cost, cell permeability and non-immunogenicity. In the past decades many Cu–Zn SOD model compounds have been reported, while very little reported work deals with iron SOD model compounds and the manganese SOD model compound^{12–15} for which crystal structures have been determined. The crystal structure of the native (oxidized form) manganese SOD, reveals that the manganese adopts a trigonal-bipyramidal co-ordination geometry with N_3O_2 ligand-donor sets,¹⁶ the three nitrogens being provided by three histidine residues in the protein. Among reported structurally characterized manganese complexes which exhibit SOD activity, only $[\text{Mn}(\text{OCH}_2\text{Ph})(\text{N}_2\text{C}_3\text{H}_2\text{Pr}^1_2-3,5)\{\text{HB}(\text{N}_2\text{C}_3\text{HPr}^1_2-3,5)_3\}]$ possesses trigonal-bipyramidal geometry.¹⁴ In our efforts to search for manganese SOD mimics, we succeeded in preparing and characterizing a new five-co-ordinate manganese(II) complex which bears structural similarities to the active sites of manganese SOD and found that it is effective for superoxide dismutation.

Experimental

Materials

Tetra-*n*-butylammonium perchlorate was twice recrystallized from absolute ethanol and dried in vacuum at 40 °C prior to use. Acetonitrile was purified as previously described.¹⁷ Nitro blue tetrazolium and methionine (B.R.) were obtained from

Sigma Co. and used as received. Riboflavin was analysed by the literature method.¹⁸ The salts KH_2PO_4 (A.R.) and K_2HPO_4 (A.R.) were recrystallized twice from deionized water. All other chemicals were reagent grade used without further purification.

Preparations

Tris(benzimidazol-2-ylmethyl)amine (ntb) was synthesized following a procedure reported previously¹⁹ with a yield of 53% and a m.p. of 270 °C.

$[\text{Mn}(\text{ntb})(\text{Hsal})][\text{ClO}_4]$. To a stirring solution of ntb (204 mg, 0.5 mmol) in methanol (20 cm³) was added $\text{Mn}(\text{ClO}_4)_2 \cdot 6\text{H}_2\text{O}$ (181 mg, 0.5 mmol) and then a solution of NaHsal (80 mg, 0.5 mmol) (H_2sal = salicylic acid) in methanol (10 cm³). The resulting clear solution was stirred for 3 h and then allowed to stand at room temperature. Light yellow crystals suitable for X-ray diffraction studies were obtained after 1 week (196 mg, yield 56%) (Found: C, 53.34; H, 3.93; Mn, 7.91; N, 14.21. Calc. for $\text{C}_{31}\text{H}_{26}\text{ClMnN}_7\text{O}_7$: C, 53.26; H, 3.75; Mn, 7.86; N, 14.03%).

CAUTION: although we experienced no difficulties with the compounds isolated as their perchlorate salts, the unpredictable behaviour of such salts necessitates extreme caution in their handling.

Crystallography

Parameters for data collection and refinement are given in Table 1. The intensities were collected at 295 K on a Siemens P₄ four-circle diffractometer with monochromated Mo-K α (λ = 0.710 73 Å) radiation using the θ – 2θ scan mode with a variable scan speed 5.0–50.0° min^{–1} in ω . The data were corrected for Lorentz-polarization effects during data reduction using XSCANS.²⁰

The structure was solved by direct methods and refined on F^2 by full-matrix least-squares methods using SHELXTL.²¹ All the non-hydrogen atoms were refined anisotropically. The hydrogen atoms were placed in calculated positions (C–H 0.96, N–H 0.90 and O–H 0.85 Å) assigned fixed isotropic thermal parameters 1.2 times the equivalent isotropic U of the atoms to which they are attached (1.5 times for the OH and methyl groups) and allowed to ride on their respective parent atoms. Their contributions were included in the structure-factor calculations.

All computations were carried out on a Pc-586 computer using the SHELXTL PC package.²¹ Analytical expressions of neutral-atom scattering factors were employed and anomalous dispersion corrections were incorporated.²²

CCDC reference number 186/865.

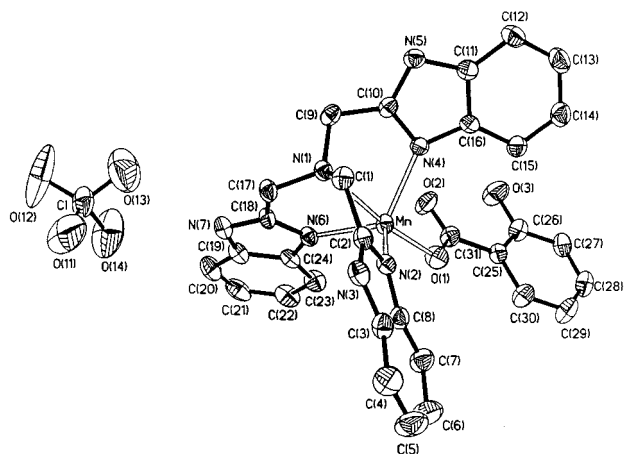


Fig. 1 Molecular structure and atom numbering of the complex with hydrogen atoms omitted for clarity. Thermal ellipsoids are drawn at the 30% probability level

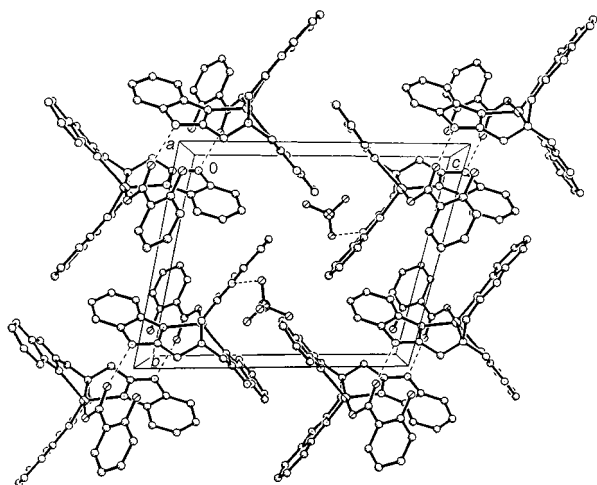


Fig. 2 Packing of the unit cell of the complex

Other physical techniques

Elemental analyses were performed on a Perkin-Elmer 240C analytical instrument. The room-temperature magnetic susceptibility data on powder samples were measured at 6000 G (0.6 T) by using a CAHN-2000 Faraday-type magnetometer. The apparatus was calibrated with $[\text{Ni}(\text{en})_3][\text{S}_2\text{O}_3]$ (en = ethane-1,2-diamine). Diamagnetic corrections were made using Pascal's constants. Cyclic voltammetry was performed on a BAS-100B electrochemical analyzer, in conjunction with a purged dinitrogen gas inlet and outlet, a glassy-carbon working electrode, a Ag–AgCl reference electrode and a platinum auxiliary electrode. All electrochemical experiments were carried out under dry and purified dinitrogen atmosphere at 298 K. The solution was 1.5×10^{-3} M in complex and 0.1 M in supporting electrolyte, NBu_4ClO_4 .

Assay of SOD activities

The SOD activities were measured according to the previously reported method.²³ The reduction of nitro blue tetrazolium was monitored at 560 nm on a Shimadzu UV-240 spectrophotometer. All photoinduced reactions were performed at 30 °C.

Results and Discussion

Crystal structure

Selected bond distances and angles are listed in Table 2,

Table 1 Crystal data and summary of data collection for the complex $[\text{Mn}(\text{ntb})(\text{Hsal})](\text{ClO}_4)$

Formula	$\text{C}_{31}\text{H}_{26}\text{ClMnN}_7\text{O}_7$
M_r	698.98
Colour/habit	Pale yellow prism
Crystal dimensions/mm	$0.40 \times 0.40 \times 0.30$
Crystal system	Triclinic
Space group	$P\bar{1}$
$a/\text{\AA}$	10.030(3)
$b/\text{\AA}$	12.563(4)
$c/\text{\AA}$	14.189(7)
$\alpha/^\circ$	99.54(3)
$\beta/^\circ$	96.96(3)
$\gamma/^\circ$	112.46(2)
$U/\text{\AA}^3$	1595.6(10)
Z	2
$D/\text{Mg m}^{-3}$	1.455
$F(000)$	718
μ/mm^{-1}	0.556
Index ranges	$0 \leq h \leq 10, -14 \leq k \leq 13, -16 \leq l \leq 16$
Reflections collected	5763
Independent reflections	5391 ($R_{\text{int}} = 0.0244$)
Absorption correction	Semiempirical from ψ scans
Data, restraints, parameters	5391, 0, 433
R, R' (observed data) [$I > 2\sigma(I)$]	0.0600, 0.1641
w^{-1}	$\sigma^2(F_o^2) + (0.080P)^2 + 0.15P^*$
Goodness of fit on F^2	1.035
$\rho_{\text{max}}, \rho_{\text{min}}/\text{e \AA}^{-3}$	1.112, -0.618
* $P = (F_o^2 + 2F_c^2)/3$.	

Table 2 Selected bond lengths (Å) and angles (°)

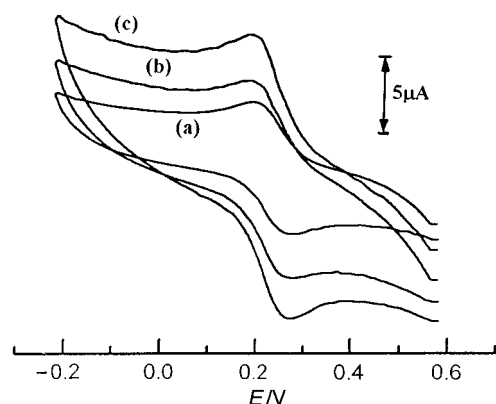
Mn–N(1)	2.508(4)	Mn–N(6)	2.124(4)
Mn–N(2)	2.146(4)	Mn–O(1)	2.035(3)
Mn–N(4)	2.176(4)	Mn...O(2)	3.181(8)
N(1)–Mn–N(2)	73.76(13)	N(4)–Mn–N(6)	123.02(14)
N(2)–Mn–N(4)	107.05(13)	N(1)–Mn–O(1)	173.46(13)
N(2)–Mn–N(6)	104.02(14)	N(4)–Mn–O(1)	101.94(14)
N(1)–Mn–N(4)	71.58(12)	N(2)–Mn–O(1)	109.7(2)
N(1)–Mn–N(6)	73.04(13)	N(6)–Mn–O(1)	110.8(2)

important hydrogen-bonding parameters in Table 3. The molecular structure of the complex is shown in Fig. 1. The crystal structure of the complex consists of discrete $[\text{Mn}(\text{ntb})(\text{Hsal})]^+$ cations and perchlorate. The Mn^{II} is five-coordinate with a N_4O ligand donor set. The ligand ntb acts as a tetradentate N-donor and the carboxylate group of the salicylate is co-ordinated to the manganese unidentately. The coordination geometry of the manganese may be best described as distorted trigonal bipyramid. The trigonal plane is occupied by the three ligating nitrogen atoms of the benzimidazolyl groups. The Mn atom protrudes toward O(1) and is 0.639 Å out of the plane. The angles N(4)–Mn–N(6), N(2)–Mn–N(4), N(2)–Mn–N(6) are 123.02(14), 107.05(13) and 104.02(14)°, respectively. The axial ligating atoms are N(1) and O(1) with Mn–N(1) 2.508(4) Å, Mn–O(1) 2.035(3) Å and N(1)–Mn–O(1) 173.46(13)°. The N(1)–Mn–N(2) 73.76(13), N(1)–Mn–N(4) 71.58(12) and N(1)–Mn–N(6) 73.04(13)° angles appear essentially imposed by the stereochemistry of the ligand ntb. The distance between Mn and O(2) is 3.181(8) Å, i.e. O(2) is not co-ordinated. The perchlorate anions and the solvent water molecules are disordered. The distorted trigonal-bipyramidal geometry of the complex is close to that known for the active site of manganese SOD.¹⁶ However, the donor set and the oxidation state of manganese are different. The manganese in the complex has a N_4O ligand donor set and is in the divalent state, while that in native manganese SOD has a N_3O_2 ligand donor set and is trivalent but can be reduced to the divalent state without any loss of enzymatic activity.²⁴

Table 3 Hydrogen-bonding parameters

X–H...Y	X...Y/Å	X–H–Y/°
N(3)–H(3)...O(12A)	2.939	145.7
N(7)–H(7)...O(14)	2.963	147.6
O(3)–H(3)...O(2)	2.597	146.4
N(5)–H(5)...O(2B)	2.838	154.6

Symmetry codes: A 2 – x, 2 – y, 1 – z; B 1 – x, 2 – y, –z.

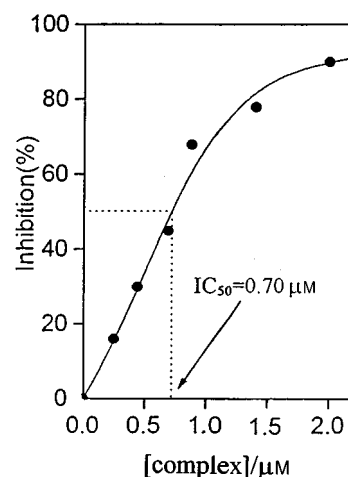
**Fig. 3** Cyclic voltammogram of a 1.5×10^{-3} M solution of the complex in MeCN (0.1 M NBu₄ClO₄) at a glassy-carbon electrode and Ag–AgCl as a reference electrode. Sweep rate: (a) 50, (b) 100 and (c) 200 mV s^{–1}. Temperature 25 °C

There is significant intermolecular hydrogen-bonding association. Two mononuclear molecules form a dimer through a couple of hydrogen-bonding bridges [N(5)–H(5)...O(2)]. Besides, each perchlorate is hydrogen bonded to N(7) of the ligand ntb in one dimer and N(3) of ntb in another [N(7)–H(7)...O(14) and N(3)–H(3)...O(12)], forming a bridge between two dimers (not shown in Fig. 2). These interactions lead to a zigzag chain structure running parallel to the crystallographic *a* axis. Additionally, the unidentate salicylate possesses an intramolecular hydrogen bond [O(3)H(3)...O(2)] and this intramolecular hydrogen bond may be an important factor in stabilizing the trigonal-bipyramidal geometry because the carbonyl group of the carboxylate is hydrogen bonded to the α -hydroxy group, thus preventing direct co-ordination of O(2).

Magnetic properties and cyclic voltammetry

The effective magnetic moment of the complex at room temperature is $5.88 \mu_B$ ($\mu_B \approx 9.27 \times 10^{-24} \text{ J T}^{-1}$) which is close to the value expected for high-spin manganese(II).

The electrochemical properties of the complex have been studied by cyclic voltammetry (CV) in dry and degassed MeCN. The cyclic voltammogram is shown in Fig. 3. There is a steeply sloping baseline due to the relatively large background current which was not deducted. The anodic peak potential E_{pa} does not vary with scanning rate and the peak-to-peak separation ($\Delta E_p = E_{pa} - E_{pc}$) of 60 mV indicates a reversible one-electron oxidation (Mn^{III}–Mn^{II}) and $E_i [(E_{pa} + E_{pc})/2]$ is equal to 0.23 V. The neutral uncomplexed ligand ntb is not electroactive over the range –0.5 to +1.0 V. According to previous reports,²⁵ for a transition-metal complex to be an effective mimic of superoxide dismutase it must have a reduction potential below 0.65 [$E^\circ(\text{}^1\text{O}_2\text{--O}_2^-)$] and above –0.33 V [$E^\circ(\text{O}_2\text{--O}_2^-)$] such that catalysis can take place but toxic singlet oxygen cannot be formed. It is known that hexaaquamanganese(II) ion is not expected to be a catalyst due to the high standard reduction potential of the couple Mn³⁺–Mn²⁺ (1.51 V). Since $E^\circ(\text{O}_2\text{--H}_2\text{O}_2)$ is 0.94 V at pH 7, the equilibrium $\text{Mn}^{2+} + 2\text{H}^+ + \text{O}_2^- \rightleftharpoons \text{Mn}^{3+} + \text{H}_2\text{O}_2$ lies to the left. Though it is unreasonable to compare the value 0.23 V with the reduction potentials of the couples $\text{O}_2\text{--O}_2^-$,

**Fig. 4** The SOD activity of the complex in the riboflavin–methionine–nitro blue tetrazolium assay

$^1\text{O}_2\text{--O}_2^-$ and $\text{O}_2^-\text{--H}_2\text{O}_2$ because the reference electrodes and solvents are different, the redox potential of the complex in water solution should be in the allowed range of a SOD mimic since the results of SOD activity assay obtained showed that it has relatively high activity (see below).

Superoxide dismutase assay

The superoxide dismutase activity of the complex was examined indirectly using the nitro blue tetrazolium assay.²³ Illumination of reaction mixtures which contained 3.4×10^{-6} M riboflavin, 0.01 M methionine, 4.6×10^{-5} M nitro blue tetrazolium, and 0.05 M potassium phosphate at pH 7.8 and at 30 °C caused an increase in absorbance at 560 nm of 0.091 min^{-1} in aerobic solutions. When the complex was added the rate of increase was reduced with increasing concentration (Fig. 4). The complex shows an IC_{50} value of $0.70 \mu\text{M}$ which indicates that it is a potent superoxide dismutase mimic. The IC_{50} value is the concentration of the complex which exerts activity equal to one unit of that of native SOD. The present value is one of the lowest for a manganese superoxide dismutase mimic and is close to the $0.75 \mu\text{M}$ reported by Kitajima *et al.*¹⁴ for a manganese(II) benzoate tris(pyrazolyl)borate complex. It is worth noting that the present complex and the benzoate tris-(pyrazolyl)borate complex both have a N₄ co-ordination sphere and lower than O_h symmetry with azine and azol types of ligands, and both possess a distorted trigonal-bipyramidal geometry which is similar to the active site of native manganese SOD. It is probable that the co-ordination of such nitrogen bases and their particular geometry leads to high superoxide dismutase activity.

References

- 1 J. K. Hurst and W. C. Barrette, jun., *Crit. Rev. Biochem. Mol. Biol.*, 1989, **24**, 271.
- 2 A. E. G. Case, in *Metalloproteins*, Part I, ed. P. Harrism, Verlag Chemie, Weinheim, 1985.
- 3 I. Fridovich, *Acc. Chem. Res.*, 1982, **15**, 200.
- 4 *Biological and Clinical Aspects of Superoxide and Superoxide Dismutase*, eds. W. H. Bannister and J. V. Bannister, Elsevier, New York, 1980.
- 5 *Free Radicals, Ageing and Applications with Superoxide Dismutase*, eds. J. E. Johnson, R. Walford, D. Harman and J. Miquel, Alan R. Liss, New York, 1986.
- 6 J. M. McCord, S. H. Sykes and K. Wong, *Adv. Inflamm. Res.*, 1979, **1**, 273.
- 7 A. Gärtner and U. Weser, *Top. Curr. Chem.*, 1986, **132**, 1.
- 8 W. Huber, M. G. P. Saifer and L. D. Williams, in *Biological and Clinical Aspects of Superoxide Dismutase*, eds. W. H. Bannister and J. V. Bannister, Elsevier, New York, 1980, vol. 11B, 395.
- 9 D. L. Darr, S. Yanni and S. Pinnel, *J. Free Radical Biol. Med.*, 1988, **4**, 357.

- 10 K. M. Faulkner, R. D. Stevens and I. Fridovich, *Arch. Biochem. Biophys.*, 1994, **310**, 341.
- 11 K. Wada, Y. Fujibayashi and A. Yokoyama, *Arch. Biochem. Biophys.*, 1994, **310**, 1.
- 12 J. Stein, J. P. Fackler, G. J. McClure, J. A. Fee and L. T. Chan, *Inorg. Chem.*, 1979, **18**, 3511.
- 13 R. Rajan, R. Rajaram, B. U. Nair, T. Ramasami and S. K. Mandal, *J. Chem. Soc., Dalton Trans.*, 1996, 2019.
- 14 N. Kitajima, M. Osawa, N. Tamura, Y. Moro-oka, T. Hirano, M. Hirobe and T. Nagano, *Inorg. Chem.*, 1993, **32**, 1879.
- 15 D. P. Riley and R. H. Weiss, *J. Am. Chem. Soc.*, 1994, **116**, 387.
- 16 W. C. Stallings, K. A. Strong and M. L. Ludwig, *J. Biol. Chem.*, 1985, **260**, 16 424.
- 17 J. F. Odonnel, J. T. Ayres and C. K. Mann, *Anal. Chem.*, 1965, **37**, 1161.
- 18 *British Pharmacopoeia*, London, HMSO, 1980, p. 1390.
- 19 L. L. Thompson, B. S. Ramaswamy and E. A. Seymour, *Can. J. Chem.*, 1977, **55**, 878.
- 20 XSCANS, Version 2.1, Siemens Analytical X-Ray Instruments, Madison, WI, 1994.
- 21 SHELXTL, Version 5.0, Siemens Industrial Automation, Analytical Instrumentation, Madison, WI, 1995.
- 22 *International Tables for X-Ray Crystallography*, Volume C (1992), ed. A. J. C. Wilson, Kluwer, Dordrecht, 1992, vol. C, Tables 6.1.1.4 (pp. 500–502), 4.2.6.8 (pp. 219–222) and 4.2.4.2 (pp. 193–199).
- 23 C. Beauchamp and I. Fridovich, *Anal. Biochem.*, 1971, **44**, 276.
- 24 J. A. Fee, E. R. Shapiro and T. H. Moss, *J. Biol. Chem.*, 1976, **251**, 6157.
- 25 W. H. Koppenol, F. Levine, T. L. Hatmaker, J. Epp and J. D. Rush, *Arch. Biochem. Biophys.*, 1986, **251**, 594.

Received 15th October 1997; Paper 7/07433F